Ceramics International 31 (2005) 1103–1107

CERAMICS INTERNATIONAL

www.elsevier.com/locate/ceramint

Morphology and growth mechanism of CVD alumina–silica

Zhaofeng Chen [a,*], Shibo Li [b], Zili Liu [a]

[a] College of Material Science and Technology, Nanjing University of Aeronautics and Astronautics, Nanjing 210016, PR China
[b] School of Mechanical and Electronic Control Engineering, Beijing Jiaotong University, Beijing 100044, PR China

Received 2 August 2004; received in revised form 18 October 2004; accepted 2 December 2004

Abstract

The purpose of the present paper is to examine the morphology and growth mechanism of the CVD alumina–silica film deposited at low temperatures and low pressure using the chemical reaction kinetics, the Gibbs–Thomson relation, solidification theory, and supersaturation condensation fusion mechanism. The dense CVD alumina–silica films were deposited on the surface of graphite paper using $AlCl_3$–$SiCl_4$–H_2–CO_2 as precursor in the temperature range of 300–550 °C. XRD and SEM were used to examine the phase composition and the microstructure of the CVD alumina–silica, respectively. The CVD alumina–silica films were composed of a large number of spherical particles accumulated by a number of fine-particles. The fusion took place among the solid particles. The spherical morphology and the fusion all resulted from the liquid droplets, which resulted from the supersaturation of the chemical reaction gaseous species in CVD alumina–silica. The liquid droplets were confirmed by comparing the morphology of the CVD alumina–silica with the typical and stable morphology of the solidified mass from liquid.

Keywords: CVD; Alumina–silica; Morphology; Growth mechanism; Liquid droplet

1. Introduction

The tendency for carbons to oxidize and become a vapor was a problem that limited the use of carbons at high temperatures. Structural carbons included carbon fibers, carbon–carbon composites and graphite. They were used in aerospace and various industrial applications. Much attention had been given to the development of methods of oxidation protection of carbon materials [1,2]. Mullite ($3Al_2O_3{\cdot}2SiO_2$), due to its thermal stability, superior corrosion resistance at high temperature, had been targeted as a prime candidate coating materials [3]. Since mullite coating by chemical vapor deposition (CVD) using $SiCl_4/AlCl_3/CO_2/H_2$ was proposed by Sarin and Mulpuri [4], a comprehensive investigation of the CVD of SiO_2, Al_2O_3 and aluminosilicate coatings from mixtures of $SiCl_4$ or CH_3SiCl_3 and AlCl3 in CO_2 and H_2 was carried out in previous studies [5–7]. However, because of the high deposition temperature (above 950 °C) and resultant strong oxidation from H_2O to carbon materials, SiC barrier layer between mullite coating and carbon material was necessary [8,9]. Even though, A SiO_2 interface resulted from the H_2O appeared between mullite and SiC coating [3]. To avoid oxidation, the mullite films always were prepared by pulsed laser deposition, electrophoresis deposition, dip-coating and sol–gel [10–12]. However, CVD has been known to be the most effective to prepare dense membranes without defects. So that it is very necessary to find a CVD method of low temperature to prepare mullite coating. The present author prepared a dense alumina–silica film on the surface of graphite paper by CVD at only 550 °C using $SiCl_4$–$AlCl_3$–CO_2–H_2, and the film could be transferred into mullite coating by heat-treatment in inert atmosphere. Morphology and growth mechanism of CVD alumina–silica coating deposited at relative low temperature has not been reported.

Compared with reactions between liquids and solids, the reactions among the gases species are more complex and difficult to control because more median reactions are involved in the CVD process. As a result, a small variation in deposition conditions contributes to the significant difference

---

* Corresponding author.
E-mail address: zhaofeng_chen@163.com (Z. Chen).

doi:10.1016/j.ceramint.2004.12.003

in both the morphology and microstructure of the deposit. Usually, the properties of the deposit are mainly dependent on the materials, which are strongly controlled by the growth behavior of the deposit.

Based on the single-layer theory, the typical CVD mechanism was developed, a mechanism usually described as follows [13,14]: (1) transport of reactant species to the vicinity of the substrate; (2) diffusion of reactant species to the substrate surface; (3) adsorption of reactant species; (4) surface diffusion, dissociation, inclusion of coating atoms into the growing surface, and formation of byproduct species; (5) de-absorption of by-product species; (6) diffusion of by-product species into the bulk gas; and (7) transport of by-product species away from the substrate (exhaust). The morphology of the thin solid film deposited at high temperatures and low atmosphere pressure was successfully explained by the above theory. However, it is difficult to interpret the morphology of the deposited film. In the typical deposition theory, the gaseous species were considered in the molecular. In fact, the gaseous species were in an ionic state because of decomposition at high temperature. The research on morphology of the deposit is usually based on the thermodynamic calculations of chemical reactions. Xu [15] proposed supersaturation condensation fusion mechanism in CVD SiC deposited at high temperatures and atmosphere pressure: the deposition obeys the typical CVD mechanism and is constrained in a very thin layer. As the deposition proceeds, the supersaturation is increased constantly, which results in the formation of liquid droplets. When the liquid droplets move toward the substrate, the fusion takes place among the liquid droplets.

The purpose of the present paper is to examine the morphology and growth mechanism of the CVD alumina–silica film deposited at low temperatures and low pressure using the chemical reaction kinetics, the Gibbs–Thomson relation, solidification theory, and supersaturation condensation fusion mechanism.

2. Experimental procedure

Alumina–silica film examined in the present study was prepared by CVD at various temperatures ranging from 300 to 550 °C using the $AlCl_3$–$SiCl_4$–H_2–CO_2 system on a graphite paper. The $AlCl_3$ evaporator was maintained at 130 °C in an oil bath. The $SiCl_4$ bubbler was maintained at 20 °C in a refrigerated bath. The gas lines from the $AlCl_3$ evaporator to the reactor were heated to 200 °C in order to prevent $AlCl_3$ from condensing. All reactant gases were mixed just before introduction into the reactor. The stoichiometry of the input $AlCl_3/SiCl_4$ mol ratio and the total pressure in the reaction chamber were fixed at 3:1 and 75 torr, respectively. The deposition time of every circle was 5 h.

The films were examined by X-ray diffraction (XRD, Rigaku D/Max-B) for phase identification using Ni-filtered Cu Kα radiation at a scanning rate of 0.5°/s and scanning from 20 to 70° of 2θ. The surface morphologies of the films were observed by scanning electronic microscopy (SEM, Model JEOL 840). The chemical compositions of the films were analyzed by energy dispersive spectroscopy (EDS, LINK-860).

3. Results and discussion

3.1. The characterization of the CVD alumina–silica film

The chemical reactions in CVD alumina–silica film are as followed.

$$H_2 + CO_2 = H_2O + CO \tag{1}$$

$$2AlCl_3 + 3H_2O = Al_2O_3 + 6HCl \tag{2}$$

$$SiCl_4 + 2H_2O = SiO_2 + 4HCl \tag{3}$$

Figs. 1 and 2 show the XRD patterns and EDS spectrum of the CVD alumina–silica film deposited onto the graphite paper at 550 °C, respectively. Because the CVD alumina–silica film was too thin to hold up the X-rays, the strong graphite peaks attributed to the graphite paper substrate were observed in the XRD patterns. These results indicate that the CVD alumina–silica film is composed of γ-alumina containing amorphous silica. According to the breadth of the diffraction peaks, the size of the γ-alumina crystals was calculated from the following Scherrer equation [16].

$$D = 0.89\lambda/\beta\cos\theta \tag{4}$$

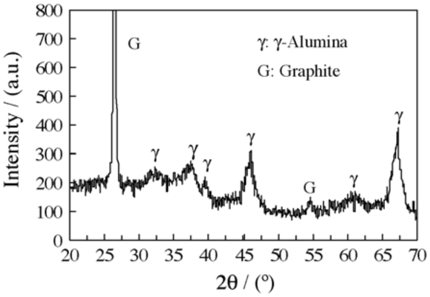

Fig. 1. XRD pattern of the CVD alumina–silica film deposited at 550 °C.

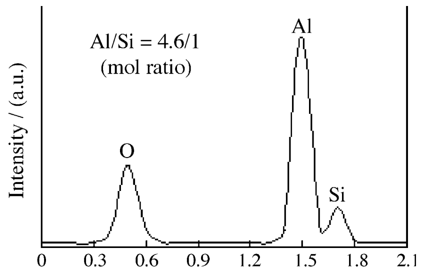

Fig. 2. EDS spectrum of the CVD alumina–silica film deposited at 550 °C.

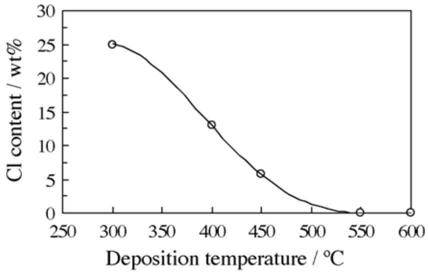

Fig. 3. Cl content in the CVD alumina–silica film deposited at different deposition temperature.

where λ is the wavelength of the characteristic X-rays, θ is the Bragg angle, and β *is* the calibrated width of the half-height of diffraction peaks. The average size of the γ-alumina crystals was about 10–20 nm.

Because the XRD patterns of the CVD alumina–silica film deposited below 550 °C show amorphous phase, by which the CVD alumina and silica cannot be distinguished, they were absent in the paper.

Fig. 3 shows the Cl content in CVD alumina–silica film deposited at different temperature. It indicates the higher the deposition temperature was, the less the Cl content in the deposit was. For the deposition temperature of 550 °C, Cl element was not observed in the film.

3.2. Morphology of the CVD alumina–silica film

Fig. 4 shows the SEM photographs of the surface morphology of the CVD alumina–silica film deposited at different deposition temperature. The micro-cracks in the texture of the film deposited at 300 °C are attributed to the difference of the thermal expansion between the CVD alumina–silica and graphite paper. The SEM photographs indicate the films are composed of a large number of spherical particles and the morphology of the CVD alumina–silica is dependent on the deposition temperature. For the deposition temperature of 400 °C, the size of the particles is smaller and more homogeneous than that deposited at 300 °C. For the deposition temperature of 550 °C, the film was dense and the size of the particles was homogenized, and hyper-particles existed in the film deposited at 300 °C were not observed.

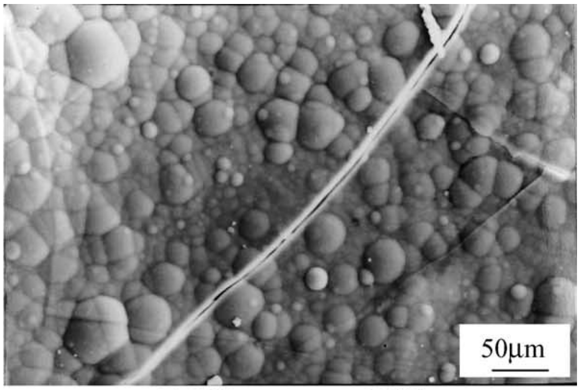

(a) CVD temperature 300°C

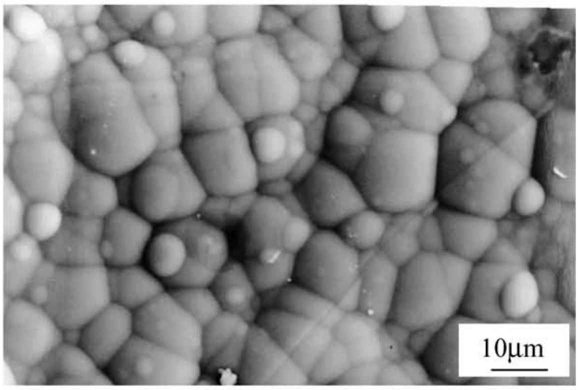

(b) CVD temperature 400°C

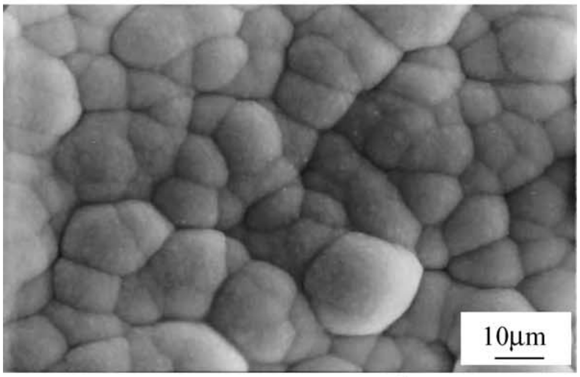

(c) CVD temperature 550°C

Fig. 4. SEM photographs of the surface of the CVD alumina–silica.

With regard to chemical reaction kinetics, CVD includes two processes, i.e., mass transport and chemical reaction of the gaseous species [17]. At low temperatures, chemical reaction is the rate limiting process, but at relatively high temperatures, the rate limiting process is shifted to mass transport. At a deposition temperature of 300 °C, the chemical reaction proceeds very slowly and the concentration of H_2O, resulting from the reaction between H_2 and CO_2, was low. As the process proceeds, the supersaturation of reactant species increases because the partial pressure of reactant species increases within the boundary layer of the graphite substrate. According to the gas dynamics [18], the condensation of the vapor would occur when the supersaturation degree reaches the critical values. The condensation in the boundary layer would lead to the formation of liquid droplets.

According to the Gibbs–Thomson relation [19], the correspondence between the size (B) of the liquid droplets and supersaturation ($\Delta\mu$) of the reactant species can be expressed by the following equation:

$$B \propto 1/\ln(\Delta\mu) \tag{5}$$

The increase of deposition temperature results in faster chemical reaction rate, and then the increase of the supersaturation of H_2O, in turn, which leads to a decrease of the size of the condensed liquid droplets. Consequently, the size of the alumina–silica particles decreased with the increase of the CVD temperature.

Because of the high activation energy required for surface diffusion at 300 °C, the complete fusion among the particles is very difficult. The resulting particles maintain the as-formed spherical morphology and there are many especially big and small particles in the alumina–silica film. The surface diffusion can carry out with the increase of the CVD temperature, so that the fusion takes place among the CVD alumina–silica particles. The dependence of the size on deposition temperature was attributed to the mobility at different temperature, that is, high deposition temperature led to high mobility of individual atoms over the particles surface and resulted in the decrease of the size of large particles, whereas low surface mobility of atoms led to heterogeneous particles size at low deposition temperature. Therefore, the size of alumina–silica particles became into homogeneous when deposition temperature was 550 °C.

In general, the chloride free-water can react with H_2O to form hydroxide colloids. Consequently, $Al(OH)_3{\cdot}xH_2O$ and $Si(OH)_4{\cdot}\,yH_2O$ colloids or their mixture, which have the spherical characteristic and can deform when adsorbing one another, must have existed in the liquid droplets. According to Fig. 3 result, the liquid droplet must have been composed of a number of colloids including Cl^-. By reason of the surface adsorption and wetting among the hydroxide colloids, the liquid droplets absorbed onto the surface of the substrate fused together like fused metal. The fusion among the CVD alumina–silica particles was observed in Fig. 4. The liquid droplets were pyrolyzed in situ to form the spherical particle. One particle should have been resulted from one liquid droplet.

The presence of liquid droplets could be confirmed by the microstructure shown in Fig. 5, which is a magnified SEM photograph of Fig. 4(c). With regard to solidification theory, the typical and stable morphology of the solidified mass from liquid is an equiaxed structure in hexagonal form. At the deposition temperature of 550 °C, the chemical reaction proceeds very rapidly and the activities of atoms are also increased further. Therefore, the liquid droplets fused completely together, and no voids were present in the deposited film. It should be noted that many fine-particles were observed on the surface of the based particles deposited at 550 °C. Therefore, each particle could be looked as an aggregate. The size of the γ-alumina crystalline calculated by Scherrer equation was about 10–20 nm, so that the fine-particles could be composed of a large of nanometer particles. The aggregates are in cauliflower form like CVD SiC [15]. Each fine-particle in the aggregate could result from each hydroxide colloid particle in the liquid droplet. Because all reactant gases were mixed just before introduction into the reactor, and the CVD processes were carried out at low pressure, the molecules of the $AlCl_3$ and $SiCl_4$ in reaction chamber must have been homogeneously mixed. Therefore, each colloid particle in the liquid droplet was the mixture of $Al(OH)_3{\cdot}xH_2O$ and $Si(OH)_4{\cdot}\,yH_2O$, in turn, each fine-particle in the aggregate was the mixture of alumina and silica. Because of the surface tension of the liquid droplets, the fine alumina–silica particles nucleated and grown in the droplet were restrained to form an aggregate.

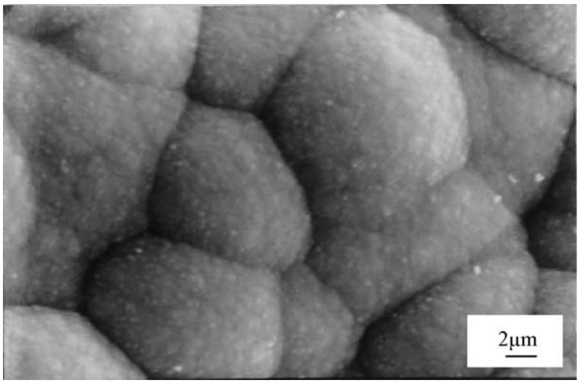

Fig. 5. The typical equiaxed morphology of the CVD alumina–silica.

4. Conclusion

(1) Morphology and growth mechanisms of the CVD alumina–silica deposited at low temperature and low pressure obey the supersaturation condensation fusion theory. As the deposition proceeds, the supersaturation of the chemical reaction gaseous species constantly increase, which results in formation of liquid droplets. The liquid droplet must have been composed of a number of $Al(OH)_3{\cdot}xH_2O$ and $Si(OH)_4{\cdot}\,yH_2O$ colloids or their mixture including Cl^-.

(2) The CVD alumina–silica film is composed of a number of spherical particles. Each particle often is composed of a number of fine-particle. The difference of the size of the CVD alumina–silica particle was reduced with increasing CVD temperature in the range of 300–550 °C. The phase composition of the CVD alumina–silica film deposited at 550 °C was γ-alumina containing amorphous silica.

(3) The spherical morphology and the fusion among the CVD alumina–silica particles all resulted from the liquid droplets. Because of the high activation energy required for surface diffusion at 300 °C, the complete fusion among the particles is very difficult. The liquid droplets were pyrolyzed in situ to form the spherical particle. As the deposition temperature increases, the activation energy of surface diffusion is reduced and the activities of atoms are increased further. Therefore, the fusion takes place among the CVD alumina–silica particles to form a dense film.

(4) Each CVD alumina–silica aggregates resulted from one liquid droplet and each fine-particle in the aggregate result from one hydroxide colloid particle in the liquid droplet.

References

[1] Y.V. Dzyadikevich, V.E. Olejnik, The ways of protection of the graphite materials against oxidation (review), Poroshkovaya Metallurgiya 34 (1996) 41–47.

[2] W. Lu, D.D.L. Chung, Oxidation protection of carbon materials by acid phosphate impregnation, Carbon 40 (8) (2002) 1249–1254.

[3] P. Hou, S.N. Basu, V.K. Sarin, Nucleation mechanisms in chemically vapor deposited mullite coatings on SiC, J. Mater. Res. 14 (7) (1999) 2952–2958.

[4] V. Sarin, R. Mulpuri, Chemical vapor deposition of mullite coatings, US Patent 5763008 (1998).

[5] S.F. Nitodas, S.V. Sotirchos, Codeposition of silica, alumina, and aluminosilicates from mixtures of CH_3SiCl_3, $AlCl_3$, CO_2, and H_2. Thermodynamic analysis and experimental kinetic investigation, Chem. Vap. Dep. 5 (1999) 219.

[6] S.F. Nitodas, S.V. Sotirchos, Chemical vapor deposition of aluminosilicates from mixtures of $SiCl_4$, $AlCl_3$, CO_2, and H_2, J. Electrochem. Soc. 147 (3) (2000) 1050–1058.

[7] S.F. Nitodas, S.V. Sotirchos, Deposition of compositionally graded mullite/alumina coatings from mixtures of $SiCl_4$, $AlCl_3$, CO_2, and H_2, Adv. Mater. 15 (6) (2003) 99–104.

[8] O. Yamamoto, T. Sasamoto, M. Inagaki, Effect of mullite coating on oxidation resistance of carbon materials with SiC-gradient, J. Mater. Sci. Lett. 19 (12) (2000) 1053–1055.

[9] J. Huang, X. Zeng, H. Li, et al. Mullite–Al_2O_3–SiC oxidation protective coating for carbon/carbon composites, Carbon 41 (14) (2003) 2825–2829.

[10] D. Tanja, J. Jelena, F. Holger, Mullite diffusion barriers on carbon based composites for high temperature applications, Annales de Chimie: Science des Materiaux 28 (Suppl. 1) (2003) S71–S78.

[11] H. Fritze, A. Schnittker, T. Witke, et al. Mullite diffusion barriers for SiC–C/C composites produced by pulsed laser deposition, Mater. Res. Soc. Symp. Proc. 555 (1999) 79–84.

[12] T. Damjanovic, H. Leipner, C. Argirusis, et al. Sol–gel route for electrophoretic deposition of mullite diffusion barriers on C/C–SiC composites, Mater. Sci. Forum 453/454 (2004) 343–348.

[13] T.M. Besmann, R.A. Lowden, D.P. Stintion, in: R. Naslain (Ed.), High Temperature Ceramic Matrix Composites, Bordeaux, Woodhead, 1993, p. 215.

[14] A.G. Suleyman, in: K.E. Spear (Ed.), Proceedings of the 11th International Conference on Chemical Vapor Deposition, American Electrochemical Society, Pennington, NJ, 1990, p. 1.

[15] Y. Xu, L. Cheng, L. Zhang, W. Zhou, Morphology and growth mechanism of silicon carbide chemical vapor deposited at low temperature and normal atmosphere, J. Mater. Sci. 34 (3) (1999) 551–555.

[16] H.P. Klug, L.E. Alexander, X-Ray Diffraction Procedures for Polycrystalline and Amorphous Materials, Wiley, New York, 1974, pp. 687–690.

[17] T.M. Besmann, B.W. Sheldon, R.A. Lowden, D.P. Stinton, Vapor-phase fabrication and properties of continuous-filament ceramic composites, Science 253 (1991) 1104B–1109B.

[18] H.W. Emmons, Fundamentals of Gas Dynamics (Section F), Princeton University Press, Princeton, 1958, p. 3.

[19] E.J. Givargiaov, Current Topics in Materials Science, North-Holland, New York, 1978, p. 91.